

# Effects of Salt on the Structure and Dynamics of the Bis(penicillamine) Enkephalin Zwitterion: A Simulation Study

Paul E. Smith and B. Montgomery Pettitt\*<sup>†</sup>

Contribution from the Department of Chemistry, University of Houston, 4800 Calhoun Road, Houston, Texas 77204-5641. Received December 19, 1990

**Abstract:** Molecular dynamics simulations of a zwitterionic bis(penicillamine) enkephalin derivative in 1.0 M saline solution have been performed. Two simulations produced essentially the same average results although they differed in the initial random placement of the salt ions. The dynamical and structural properties from the simulations were compared with those from a previous simulation of the peptide in pure water. The properties of the sodium and chloride ions were compared with those from a simulation of bulk salt solution. An inner-sphere complex between the peptide and the chloride ions was observed in which two to three chloride ions were associated with the  $\text{NH}_3^+$  terminal hydrogen atoms. Several chlorides associated with more than one amide hydrogen simultaneously, and the resulting close chloride–chloride ion contacts were additionally stabilized by bridging water molecules. The sodium ions did not associate directly with the peptide but formed an outer-sphere complex surrounding the peptide–chloride ion complex. The effect of chloride ion association on the structure and dynamics of the peptide was investigated in detail. The spatial correlations between salt ions and the enkephalin derivative are discussed in relation to  $\delta$ -opioid receptor binding. The implications that the observed ion effects have on our understanding of the Hofmeister series are also considered.

## I. Introduction

The influence of salt on the conformation and physical properties of biomolecules in solution is an essential factor which is often overlooked in the analysis of structure-activity relationships. The addition of different salts to a peptide in solution not only helps to screen the Coulombic interactions between charged groups on the peptide but can, by specific associations, alter its conformation and/or solubility.<sup>1,2</sup> The salting in and salting out of peptides in solution<sup>2</sup> and the denaturation of proteins<sup>1,3,4</sup> are two very important effects which have been investigated extensively by experiment. Although many trends have been observed, the exact nature of the underlying processes are still not known or fully understood. Differences in the cation or anion charges as well as their relative sizes and polarizability have important consequences on the solvation of ions by water<sup>5–7</sup> and the resulting interactions with solvated biomolecules.<sup>8</sup> These differences are expressed in the famous lyotropic, or Hofmeister series,<sup>9,10</sup> where the effect of ions are ordered by their ability to denature a protein or to increase or decrease the solubility of a peptide in solution.

Although the relative ability of ions to affect peptide conformation and solubility has been known for a long time, very little atomic detail is known about the stabilizing or destabilizing interactions which are important in explaining the observed effects. Flanagan et al.<sup>4</sup> have investigated the effect of bound chloride ions on the energetics of dimer–tetramer assembly in human hemoglobin and used their results to suggest a mechanism for electronic communication with the heme. Central to their calculations was the observation of a chloride ion bound between the  $\alpha$ -amino group of Val 1 $\alpha$  and the  $\beta$ -hydroxyl group of Ser 131 $\alpha$  in the crystal structure of human hemoglobin A.<sup>11</sup> Other work has suggested that both anion<sup>2,10</sup> and cation<sup>12–14</sup> effects are equally dominant. Although cations, and less often anions, are often included in simulations of DNA, these are usually not of specific interest in themselves (for a recent review see ref 15).

In addition, it is known that crystal structures of small peptides crystallized from salt solution contain anions and cations, along with water molecules, which are specifically bound to the peptide group or an ionic center.<sup>12,16–18</sup> It therefore seems possible that, in addition to the well-known Debye–Hückel screening displayed by ions, there may be specific binding sites within peptides which, when occupied, could have a dramatic effect on the solution conformation of the peptide. In order to investigate the effects of added salt on peptide conformation and dynamics, we have used the computational technique of molecular dynamics to simulate a model structure of a small peptide in explicit water and in the

presence of added sodium and chloride ions. The simulations represent approximately 1.0 M sodium chloride, which is higher than physiological saline concentration (0.15 M) but desirable to ensure statistical significance. We were particularly interested in any ion induced conformational changes and any strong correlations between the ions and the ionic moieties of the peptide.

Molecular dynamics simulations of proteins which include explicit counterions have been performed previously. Berendsen et al.<sup>19</sup> included 24 chloride counterions in their simulation of the unit cell of pancreatic trypsin inhibitor (PTI), a positively charged protein at neutral pH. They observed a range of chloride ion self-diffusion constants dependent on the interaction between the chloride ions and PTI. They also observed that the PTI appeared to stabilize water molecules in the first solvation shell of the chloride ions. Avbelj et al.<sup>20</sup> have recently completed a large simulation of *Streptomyces griseus* protease A in its ionic crystalline environment. This simulation included 26 dihydrogen phosphate ions and 16 sodium ions. The use of explicit counterions

- (1) von Hippel, P. H.; Schleich, T. *Acc. Chem. Res.* **1969**, *2*, 257–265.
- (2) Robinson, D. R.; Jencks, W. P. *J. Am. Chem. Soc.* **1965**, *87*, 2470–2479.
- (3) Franks, F.; Eagland, D. *C.R.C. Crit. Rev. Biochem.* **1975**, *3*, 165–219.
- (4) Flanagan, M. A.; Ackers, G. K.; Matthew, J. B.; Hanania, G. I. H.; Gurd, F. R. N. *Biochemistry* **1981**, *20*, 7439–7449.
- (5) Bockris, J. O.; Reddy, A. K. N. *Modern Electrochemistry*; Plenum Press: New York, 1970; Vol. 1.
- (6) Rasaiah, J. C.; Friedman, H. L. *J. Chem. Phys.* **1968**, *48*, 2742–2756.
- (7) Rasaiah, J. C. *J. Chem. Phys.* **1972**, *56*, 3071–3085.
- (8) Wood, R. H.; Wicker, R. K.; Kreis, R. W. *J. Phys. Chem.* **1971**, *75*, 2313–2318.
- (9) Hofmeister, F. *Arch. Exp. Pathol. Phar.* **1888**, *24*, 247–260.
- (10) Collins, K. D.; Washabaugh, M. L. *Q. Rev. Biophys.* **1985**, *18*, 323–422.
- (11) O'Donnel, S.; Mandaro, R.; Schuster, T. M.; Arnone, A. *J. Biol. Chem.* **1979**, *254*, 12204–12208.
- (12) Bello, J.; Haas, D.; Bello, H. R. *Biochemistry* **1966**, *5*, 2539–2548.
- (13) Roux, M.; Bloom, M. *Biochemistry* **1990**, *29*, 7077–7089.
- (14) Schleich, T.; Gentzler, R.; von Hippel, P. H. *J. Am. Chem. Soc.* **1968**, *90*, 5954–5960.
- (15) Anderson, C. F.; Record, M. T. *Ann. Rev. Biophys. Biophys. Chem.* **1990**, *19*, 423–465.
- (16) Koetzle, T. F.; Golic, L.; Lehmann, M. S.; Verbist, J. J.; Hamilton, W. C. *J. Chem. Phys.* **1974**, *60*, 4690–4696.
- (17) Frey, M. N.; Koetzle, T. F.; Lehmann, M. S.; Hamilton, W. C. *J. Chem. Phys.* **1973**, *58*, 2547–2556.
- (18) Sequeira, A.; Rajagopal, H.; Chidambaram, R. *Acta. Crystallogr.* **1972**, *B28*, 2514–2519.
- (19) Berendsen, H. J. C.; van Gunsteren, W. F.; Zwinderman, H. R. J.; Guertsen, R. G. *Ann. N. Y. Acad. Sci.* **1986**, *482*, 269–286.
- (20) Avbelj, F.; Moul, J.; Kitson, D. H.; James, M. N. G.; Hagler, A. T. *Biochemistry* **1990**, *29*, 8658–8676.

<sup>†</sup> Alfred P. Sloan fellow 1989–1991.

required an unusually large cutoff distance (15 Å) to account for the significant long-range protein-ion interactions.<sup>20</sup> Such simulations demonstrate that the inclusion of explicit counterions in molecular dynamics simulations can considerably alter the protein solution environment properties.

The zwitterionic pentapeptide Tyr-c[D-Pen-Gly-Phe-D-Pen], or DPDPE, is a cyclic enkephalin derivative with high potency and  $\delta$  opioid receptor selectivity.<sup>21-23</sup> DPDPE has been studied extensively by NMR,<sup>23-25</sup> molecular modeling,<sup>23,24,26</sup> and molecular dynamics<sup>24,27,28</sup> techniques. The peptide is thought to fold into a family of amphiphilic structures with the carbonyls on one face and the amide hydrogens on the other face of the macrocycle.<sup>24,27</sup> These conformations are stabilized by favorable interactions with surrounding water molecules.<sup>27</sup> If the effect of salt on the solution conformation of DPDPE were profound, it could prove to be an important factor in the mechanism of interaction between the peptide and the  $\delta$  opioid receptor.

In section II we present the methodology and details of the saline-peptide simulations. Section III contains the results and a discussion of the effect of added salt on the physical and chemical properties of DPDPE in solution. The conclusions are presented in section IV.

## II. Method

Two simulations were performed for DPDPE in approximately 1.0 M sodium chloride solution. The only differences between the two simulations were the initial positions of the sodium and chloride ions therefore ensuring that any results were independent of the starting configuration chosen. Initial starting positions were chosen by randomly replacing water molecules by either sodium or chloride ions. The saline-peptide simulations were performed in a cubic box of length 24.17 Å containing DPDPE, 411 water molecules, 9 sodium ions, and 9 chloride ions. A previous molecular dynamics simulation of DPDPE<sup>27</sup> with 429 water molecules in a cubic box of length 24.17 Å was used for comparison with the saline-peptide simulations. The water-water potential energy reflects the total Ewald energy including the self-energy which was not included in the tabulation in ref 27. The same initial conformation of DPDPE<sup>24</sup> was used in all three simulations.

We used the same peptide and peptide-water model and parameters as in the previous aqueous simulation.<sup>27</sup> Ion-water parameters were taken from previous work.<sup>29</sup> The  $\sigma$  and  $\epsilon$  Lennard-Jones parameters for sodium and chloride ions were extracted from the sodium-water and chloride-water parameters, respectively, and then used to calculate the DPDPE-ion interactions. This gave values of  $\sigma_{\text{Na}} = 2.22$  Å,  $\sigma_{\text{Cl}} = 3.88$  Å,  $\epsilon_{\text{Na}} = 0.6305$  kJ mol<sup>-1</sup>, and  $\epsilon_{\text{Cl}} = 4.5551$  kJ mol<sup>-1</sup>. Ion-ion interactions were modeled with a Born-Huggins-Mayer potential with parameters taken from ref 29. We used a flexible SPC model<sup>30</sup> for the water solvent with a correspondingly conservative time step of 0.5 fs and the velocity Verlet algorithm for the integration of the equations of motion. All electrostatic interactions were calculated with the Ewald procedure<sup>31,32</sup> thereby avoiding the problems associated with the use of electrostatic cutoffs. More details of our implementation of the Ewald procedure for these calculations can be found in the appendix.

Initial velocities were assigned from a Maxwell-Boltzmann distribution at 300 K. The system was allowed to evolve for 20 ps with inter-

mittent reassignment of velocities. A further 80 ps of equilibration were then performed in the microcanonical (NVE) ensemble. Finally, 100 ps of production were performed making a total of 200 ps for each of the saline-peptide systems. Further details of the simulations of DPDPE in aqueous solution can be found in ref 27.

We also performed a molecular dynamics simulation of 1.0 M sodium chloride solution in order to compare our model with other literature studies and to act as a control for the DPDPE in saline solution simulations. This system contained a total of 466 water molecules, 9 sodium ions, and 9 chloride ions in a cubic box of length 24.17 Å. We used the same ion-water potentials and parameters as used in the two saline-peptide simulations. After initial velocity assignment at 300 K the system was allowed to evolve for 20 ps with intermittent velocity reassignment. A further 30 ps of equilibration were then performed followed by 50 ps of production. Throughout the rest of this paper we will refer to the simulation of DPDPE/H<sub>2</sub>O as the aqueous DPDPE simulation, the simulations of DPDPE/H<sub>2</sub>O/NaCl as the saline-peptide simulations ions 1 and ions 2, and the simulation of H<sub>2</sub>O/NaCl as the pure salt simulation.

Electrostatic potential energy plots were obtained with the linearized Poisson-Boltzmann equation<sup>33,34</sup> solved for the same OPLS charge distribution<sup>35</sup> with a 50 × 50 × 50 grid with a 0.75-Å grid spacing. The interior and exterior dielectrics were set at 2.0 and 78.0, respectively. The atomic radii were taken from ref 36 and are consistent with single ion solvation calculations.<sup>37</sup>

## III. Results and Discussion

(a) **Ion Binding to DPDPE.** A structural analysis by inspection was performed to locate effects caused by specific associations. The striking result from the analysis of the saline-peptide simulations was the presence of several close associations between the peptide and the chloride ions. In fact, all the chloride ions were found in close proximity (contact or solvent-separated minima) to either the N terminus or the other amide hydrogens. This effect was observed in both simulations even though the chloride ions were placed at different, random, initial starting positions. Within the first 50 ps of equilibration in both simulations the majority of the chloride ions were associated with the peptide forming what may be essentially characterized as inner coordination sphere complexes.

The anionic association occurred on the surface of the peptide which had several amide hydrogens pointing in the same direction.<sup>24,27</sup> This configuration of peptide dipoles, forming a propensity for an amphiphilic structure, was previously found to be stabilized by high dielectric solvent.<sup>27</sup> The interaction between the amide dipoles and the chloride ions is such that the parallel arrangement of amide dipoles was further stabilized by coordination of chloride ions. The association process between DPDPE and the chloride ions is illustrated in Figure 1 which shows the average distance between the ions and the ionic groups of the peptide and between the ions themselves as a function of time. The result is representative of both saline-peptide simulations. The same initial average distances calculated for all the pairs ( $\approx 12$  Å) illustrates the initial random ion positioning. Also included in Figure 1c are the corresponding average distances found in the pure salt simulation. In both saline-peptide simulations the average N<sup>+</sup>-Cl<sup>-</sup> distance decreased sharply during the first 50 ps as several chloride ions approached the positively charged N terminus. The average distance then remained fairly constant for the rest of the simulation. On the other hand, the sodium ions did not associate with the negatively charged carboxylate group. In fact, the average O<sup>-</sup>-Na<sup>+</sup> distance increased slightly. This increase, being opposite to that expected, may be a consequence of the lattice nature of the Ewald calculation.

The corresponding salt ion-ion averages (Figure 1b) also show trends opposite to those expected for like and unlike charges in

(21) Mosberg, H. I.; Hurst, R.; Hruba, V. J.; Yamamura, K. G. H. I.; Galligan, J. J.; Burks, T. F. *Proc. Natl. Acad. Sci. U.S.A.* **1983**, *80*, 5871-5874.

(22) Hruba, V. J. In *Opioid Peptides: Medicinal Chemistry*; Rapaka, R. S., Barnett, G., Hawks, R. L., Eds.; NIDA Research Monograph 69, Rockville, 1986; pp 128-147.

(23) Hruba, V. J.; Pettitt, B. M. In *Computer-Aided Drug Design: Methods and Applications*; Perun, T. J., Propst, C. L., Eds.; Marcel Dekker: New York, 1989; pp 405-460.

(24) Hruba, V. J.; Kao, L.; Pettitt, B. M.; Karplus, M. *J. Am. Chem. Soc.* **1988**, *110*, 3351-3359.

(25) Mosberg, H. I.; Sobczyk-Kojiro, K.; Subramanian, P.; Crippen, G. M.; Ramalingam, K.; Woodward, R. W. *J. Am. Chem. Soc.* **1990**, *112*, 822-829.

(26) Nikiforovich, G. V.; Balodis, J.; Shenderovich, M. D.; Golbraikh, A. *Int. J. Pept. Protein Res.* **1990**, *36*, 67-78.

(27) Smith, P. E.; Dang, L. X.; Pettitt, B. M. *J. Am. Chem. Soc.* **1991**, *113*, 67-73.

(28) Pettitt, B. M.; Matsunaga, T.; Al-Obeidi, F.; Gehrig, C.; Hruba, V. J.; Karplus, M. *Biophys. J.* Submitted for publication.

(29) Pettitt, B. M.; Rosky, P. J. *J. Chem. Phys.* **1986**, *84*, 5836-5844.

(30) Dang, L. X.; Pettitt, B. M. *J. Phys. Chem.* **1987**, *91*, 3349-3354.

(31) Ewald, P. *Ann. Physik.* **1921**, *64*, 253-287.

(32) de Leeuw, S. W.; Perram, J. W.; Smith, E. R. *Proc. R. Soc. London A* **1980**, *373*, 27-56.

(33) Davis, M. E.; Madura, J. D.; Luty, B. A.; McCammon, J. A. *Comp. Phys. Comm.* **1991**, *62*, 187-197.

(34) Davis, M. E.; Madura, J. D.; Sines, J.; Luty, B. A.; Allison, S. A.; McCammon, J. A. *Methods Enzymol.* In press.

(35) Jorgensen, W. L.; Tirado-Rives, J. *J. Am. Chem. Soc.* **1988**, *110*, 1657-1666.

(36) Jarvis, L.; Huang, C.; Ferrin, T.; Langridge, R. *UCSF MIDAS User's Manual*; 1986.

(37) Mohan, V.; Davis, M. E.; Mad

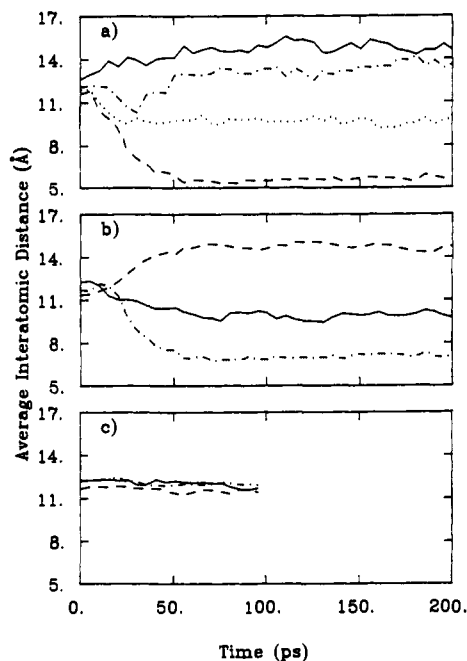


**Figure 1.** Average interatomic distances as a function of time: (a) between ions and the charged centers of the peptide, (solid line)  $\text{N}^+-\text{Na}^+$ , (dot-dashed line)  $\text{O}^--\text{Na}^+$ , (dotted line)  $\text{O}^--\text{Cl}^-$ , and (dashed line)  $\text{N}^+-\text{Cl}^-$  from one of the saline-peptide simulations; (b) between different ions in one of the saline-peptide simulations, (solid line)  $\text{Na}^+-\text{Na}^+$ , (dot-dashed line)  $\text{Cl}^- - \text{Cl}^-$ , and (dashed line)  $\text{Na}^+-\text{Cl}^-$ ; (c) ion-ion average distances from the pure salt simulation, (solid line)  $\text{Na}^+-\text{Na}^+$ , (dot-dashed line)  $\text{Cl}^- - \text{Cl}^-$ , and (dashed line)  $\text{Na}^+-\text{Cl}^-$ .

the gas phase. The trends expected in pure salt solution are those observed in Figure 1c. An effect of the strong peptide-chloride ion attraction was a lowering of the average  $\text{Cl}^- - \text{Cl}^-$  distance. The solvent averaged effective attraction between the chloride ions and the peptide was found to be stronger than the mutual repulsion between chloride ions. The  $\text{Na}^+-\text{Na}^+$  average distance was found to be roughly twice that of the chloride pairs as the sodium ions drifted away from both the peptide and the chloride ions. No tight sodium-chloride ion pairs were observed in either saline-peptide simulation although many solvent-separated chloride-chloride ion pairs were found in the vicinity of the N terminus of DPDPE. The pure salt simulation displayed no such variations in the average distances and produced no observable like or unlike ion pairs during the 100 ps of simulation. This suggests that the peptide induces and mediates the formation of several chloride-chloride ion pairs and that such ion pair formation is not a direct consequence of the parameters or model used. While certain aqueous ionic solution Hamiltonians are known to produce significant ion pairing at infinite dilution, even for some like ion pairs, both our pure salt simulation and finite concentration theories indicate that such like ion pairing can become less probable at somewhat higher concentrations.<sup>29,38-40</sup>

Examination of the final peptide and salt configurations from each of the saline-peptide runs showed them to be remarkably similar. In both cases the sodium ions surrounded the peptide-chloride ion complex and appeared to have no specific association with either. The chloride ions were found in the vicinity of the amide hydrogens and the N terminus. Each of these amide groups had a direct hydrogen-bonding interaction with either one chloride ion or a water molecule in contact with a chloride ion. A particularly striking observation was the presence of two to three chloride ions directly bound to, or closely associated with, the hydrogens on the N terminus. These chlorides had replaced the tightly bound water molecules observed in the aqueous simula-

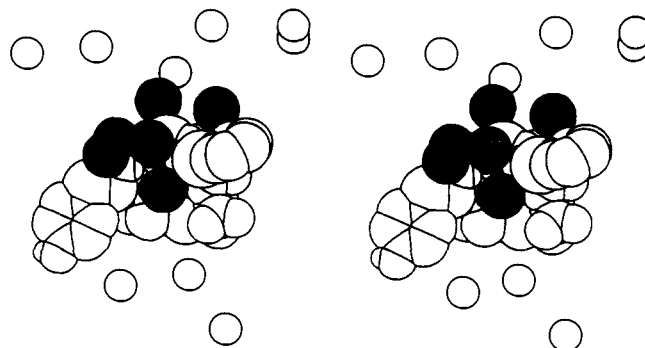


**Figure 2.** The structure of DPDPE and the arrangement of chloride ions around DPDPE after 200 ps of saline-peptide simulation. Six chloride ions (shaded spheres) and nine sodium ions (open spheres) are visible.

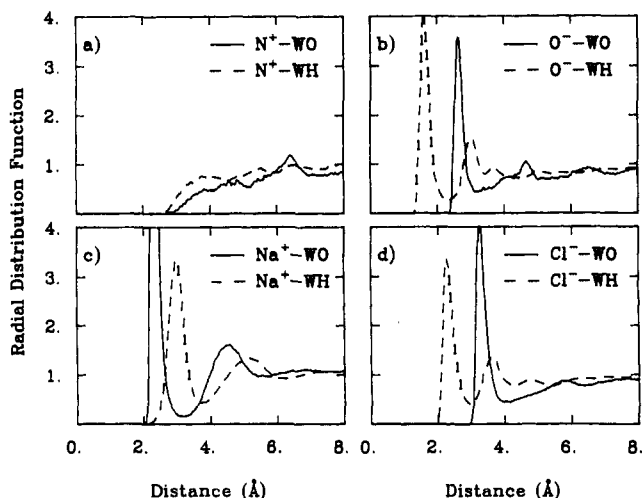


**Figure 3.** Radial distribution functions calculated from one of the saline-peptide simulations: (a)  $\text{N}^+$  and (b)  $\text{O}^-$  termini of DPDPE and (c)  $\text{Na}^+$  and (d)  $\text{Cl}^-$  ions, where WO = water oxygen and WH = water hydrogen.

tion.<sup>27</sup> One of the final configurations is shown in Figure 2. In both cases we observed one or two chloride ions which associated with the N terminal hydrogens and backbone amide hydrogens simultaneously; however, no ions were found which interacted directly with the carboxylate terminus via an inner-sphere complex.

Figure 3 shows the peptide-water and ion-water radial distribution functions (rdfs) obtained from one of the saline-peptide simulations. In nearly all comparable cases the peptide rdfs were the same in saline solution as they were in aqueous solution. The only differences occurred for rdfs to the N terminus of DPDPE. In the aqueous DPDPE simulation, water oxygens hydrogen bond to each of the hydrogens of the ammonium group.<sup>27</sup> In the saline-peptide simulations these waters were displaced by chloride ions. Hence the structure of the first peak in the  $\text{N}^+-\text{WO}$  and  $\text{N}^+-\text{WH}$  rdfs is lost. This is shown in Figure 3a. The  $\text{O}^--\text{WO}$  and  $\text{O}^--\text{WH}$  rdfs are essentially identical with those found in the aqueous simulation indicating the small, if any, correlations between the carboxylate terminus and the salt ions. Further information from the rdfs is given in Table I. The sodium-water structure and coordination numbers were in good agreement with previous results.<sup>29,38,41-44</sup> The chloride ion coordination numbers were slightly lower than those obtained for infinitely dilute chloride ions in water with the same model and parameters.<sup>38</sup> This can be explained by competition between the polar amide hydrogens and the water molecules for ion coordination. That is to say there

(41) Chandrasekhar, J.; Spellmeyer, D. C.; Jorgensen, W. L. *J. Am. Chem. Soc.* **1984**, *106*, 903-910.

(42) Guardia, E.; Padro, J. A. *J. Phys. Chem.* **1990**, *94*, 6049-6055.

(43) Cieplak, P.; Kollman, P. J. *J. Chem. Phys.* **1990**, *92*, 6761-6767.

(44) Impey, R. W.; Madden, P. A.; McDonald, I. R. *J. Phys. Chem.* **1983**, *87*, 5071-5083.

(38) Dang, L. X.; Pettitt, B. M. *J. Phys. Chem.* **1990**, *94*, 4303-4308.

(39) Buckner, J. K.; Jorgensen, W. L. *J. Am. Chem. Soc.* **1989**, *111*, 2507-2516.

(40) Kusalik, P. G.; Patey, G. N. *J. Chem. Phys.* **1988**, *88*, 7715-7738.

Table I. Radial Distribution Functions<sup>a</sup>

simulation	g (r)	peak positions	integrated to	coordination no.
DPDPE <sup>b</sup>	WO-WO	2.75, 4.61	3.23	3.9
	WO-WH	1.02, 1.76, 3.26	1.22, 2.43	2.0, 3.8
	WH-WH	1.60, 2.40, 3.90	1.79, 2.98	1.0, 6.2
	N <sup>+</sup> -WO	2.69	3.52	3.8
	N <sup>+</sup> -WH	3.42	4.10	9.8
	O <sup>-</sup> -WO	2.62	3.30	3.2
	O <sup>-</sup> -WH	1.60, 3.04	2.37	3.0, 9.0
	WO-WO	2.72, 4.58	3.39	4.4
	WO-WH	0.99, 1.73, 3.23	1.22, 2.40	2.0, 3.9
	WH-WH	1.60, 2.37, 3.87	1.76, 2.98	1.0, 6.1
ions 1	N <sup>+</sup> -WO			
	N <sup>+</sup> -WH			
	O <sup>-</sup> -WO	2.62, 4.61	3.04	2.9
	O <sup>-</sup> -WH	1.60, 2.98, 3.71	2.24, 3.39	3.0, 9.0
	Na <sup>+</sup> -WO	2.30, 4.48	3.23, 5.57	5.7, 24.4
	Na <sup>+</sup> -WH	3.01, 5.15	3.71, 6.24	14.0, 62.9
	Cl <sup>-</sup> -WO	3.26, 5.76	4.00, 6.30	6.7, 23.5
	Cl <sup>-</sup> -WH	2.27, 3.58, 4.74	2.94, 4.19, 5.31	5.8, 16.8, 32.6
	Na <sup>+</sup> -WO	2.30, 4.51	3.14, 5.44	5.8, 24.0
	Na <sup>+</sup> -WH	2.98, 5.15	3.71, 6.24	14.5, 68.0
salt	Cl <sup>-</sup> -WO	3.26, 4.96	3.94, 6.08	8.1, 30.1
	Cl <sup>-</sup> -WH	2.30, 3.68	2.98, 4.16	7.2, 20.1

<sup>a</sup>WO = water oxygen, WH = water hydrogen. <sup>b</sup>Reference 27.

is a strong three-body correlation involving the peptide. In addition, the peptide-solvent rdfs at intermediate range (4–8 Å) display physical shielding due to the presence of the sizable peptide solute.<sup>45</sup> Our water-water rdfs (Table I and ref 27) are in excellent agreement with a recent simulation of SPC water with Ewald electrostatics.<sup>46</sup> Statistically meaningful ion-ion rdfs could not be obtained due to the small number of ions in the simulation.<sup>47</sup>

In an attempt to explain the association of chloride ions with the peptide, we have calculated the electrostatic potential energy for the peptide in a plane in the vicinity of DPDPE surrounded by an aqueous dielectric continuum. The electrostatic potential energy for the initial conformation of DPDPE is shown in Figure 4. The electrostatic potential energy is very similar to that expected for a simple dipole with point charges situated at the N and C termini. The figure clearly shows that DPDPE has a large positive region in the vicinity of the N terminus. This region is attractive with respect to chloride ions, and it is to this region that several chlorides bind in our simulations. We also calculated the electrostatic potential energy for the final configuration (shown in Figure 2) with and without ions. These are shown in Figures 5 and 6 together with the projected positions of the sodium and chloride ions. The electrostatic potential energy generated by the final conformation of DPDPE without the inclusion of ions (Figure 5) still displays similar positive and negative regions to those observed for the initial structure (Figure 4), even though there is an ion induced conformational change (see next section). On inclusion of the sodium and chloride ions we observe a negative region surrounding the peptide and chlorides which is neutralized at larger distances by the presence of the sodium ions. While this helps to explain the initial attraction between the peptide and chloride ions it does not, however, explain the absence of any peptide-sodium association especially at the negatively charged C terminus. The effect of preferential ion associations is inexplicable at this continuum level of model and theory.

This anomaly was elucidated by the calculation of several pair energy distributions. In Figure 7a we show the ion-water pair distributions obtained from the pure salt simulation. From this we can assign an average binding energy between an ion and a water molecule. In the case of sodium, this is -101 kJ mol<sup>-1</sup> compared with -53 kJ mol<sup>-1</sup> for chloride. Integration of the distributions from -∞ to -50 and -35 kJ mol<sup>-1</sup> gave 5.3 and 6.8 water molecules for sodium and chloride ions, respectively. These values are close to those obtained from the rdfs in Table I and in reasonable agreement with previous calculations with other

## DPDPE ELECTROSTATIC POTENTIAL

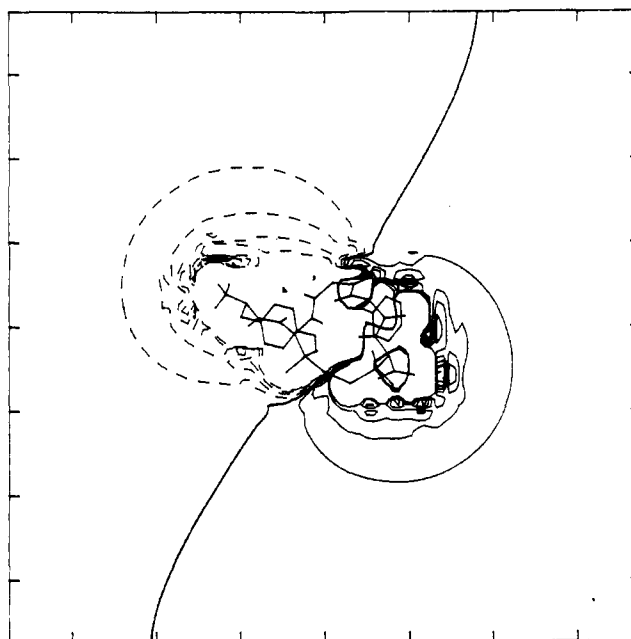


Figure 4. The electrostatic potential energy around DPDPE in its initial conformation. The thick contour is 0.0 kJ mol<sup>-1</sup>, negative (solid) contours range from -2.0 to -8.0 kJ mol<sup>-1</sup> toward the peptide while positive (dashed) contours range from 2.0 to 8.0 kJ mol<sup>-1</sup> in toward the peptide. Contours are in the plane joining the N and C termini. The atoms of the peptide are projected onto this plane.

## DPDPE ELECTROSTATIC POTENTIAL

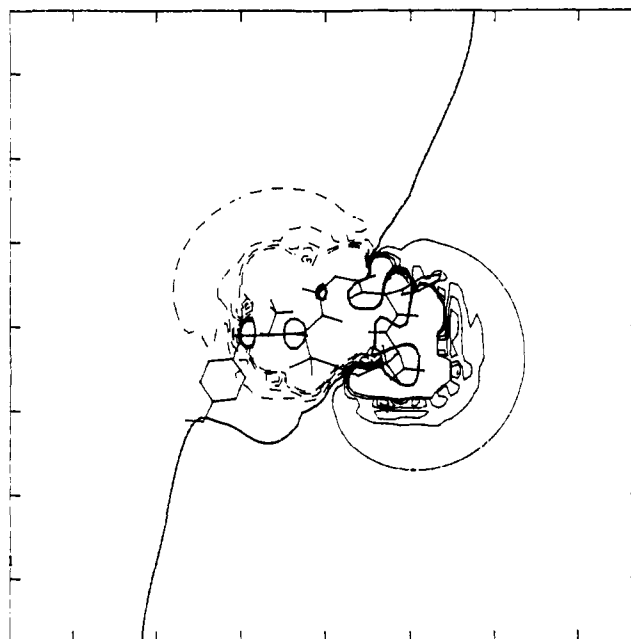


Figure 5. The electrostatic potential around DPDPE in the conformation shown in Figure 2. Contours are the same as in Figure 4.

variations on the ion force field.<sup>39,41,43,48</sup> In comparison, the corresponding pair distributions calculated from the saline-peptide simulations (not shown) gave peaks at -101 and -55 kJ mol<sup>-1</sup> for sodium and chloride. Integration to the minima at -52 and -38 kJ mol<sup>-1</sup> gave 5.1 and 5.4 water molecules, respectively. Hence the solvent structure around the sodium ions is essentially unchanged, whereas that surrounding the chloride ions has been disrupted by coordination to the peptide. The above difference

(45) Pettitt, B. M.; Karplus, M. *Chem. Phys. Lett.* **1987**, *136*, 383-386.

(46) Prevost, M.; van Belle, D.; Lippens, G.; Wodak, S. *Mol. Phys.* **1990**, *71*, 587-603.

(47) Card, D. N.; Valleau, J. P. *J. Chem. Phys.* **1970**, *52*, 6232-6240.

(48) Gao, J.; Garner, D. S.; Jorgensen, W. L. *J. Am. Chem. Soc.* **1986**, *108*, 4784-4790.

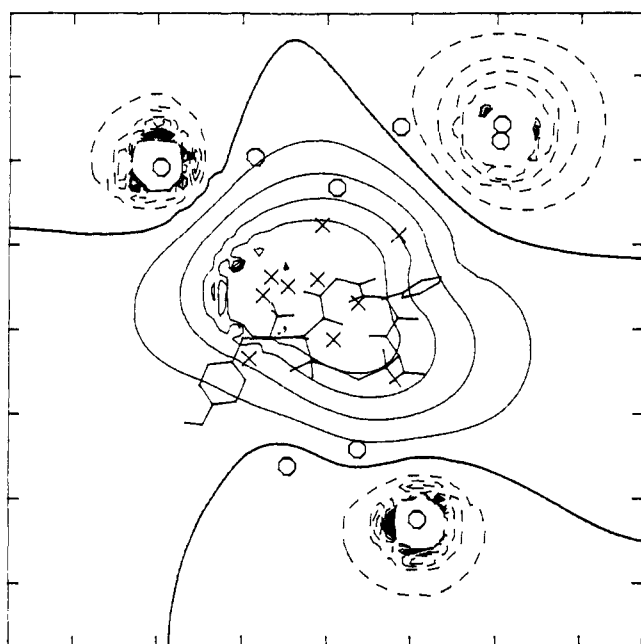
DPDPE + Na<sup>+</sup> + Cl<sup>-</sup> ELECTROSTATIC POTENTIAL

Figure 6. The same as Figure 6 except for the inclusion of sodium and chloride ions. Contours are the same as in Figure 4. Chloride ions (X) and sodium ions (O) are shown projected onto the contour plane.

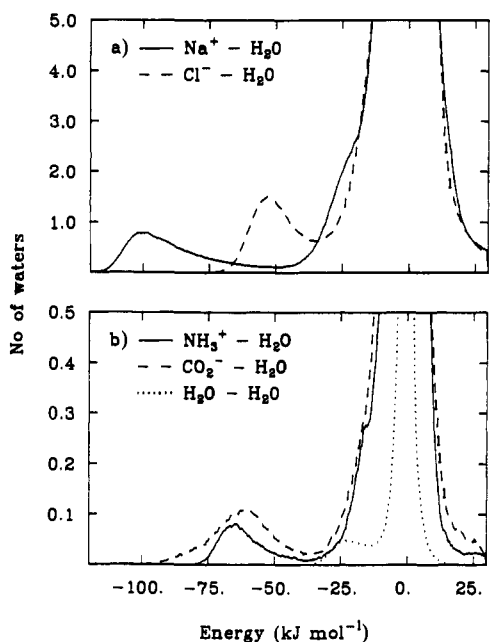


Figure 7. (a) Ion-water pair energy distributions from the pure salt simulation and (b) DPDPE-water pair energy distributions from the aqueous DPDPE simulation.

between the pure salt and saline-peptide simulations is the same as that observed in the chloride-water rdfs (Table I). In Figure 7b the pair distributions for the N and C termini obtained from the aqueous simulation are shown. We obtained interaction energies of  $-65$  and  $-60$   $\text{kJ mol}^{-1}$  for the N and C termini, respectively. These values are in good agreement with previous simulations of the related molecules  $\text{MeNH}_3^+$  and  $\text{MeCO}_2^-$  ( $-55$  and  $-63$   $\text{kJ mol}^{-1}$ , respectively).<sup>49</sup> Unfortunately it is not possible to calculate the two remaining pair distributions of importance (N terminus to chloride and C terminus to sodium) with reasonable accuracy from these simulations due to insufficient sampling.

(49) Jorgensen, W. L.; Gao, J. *J. Phys. Chem.* 1986, 90, 2174-2182.

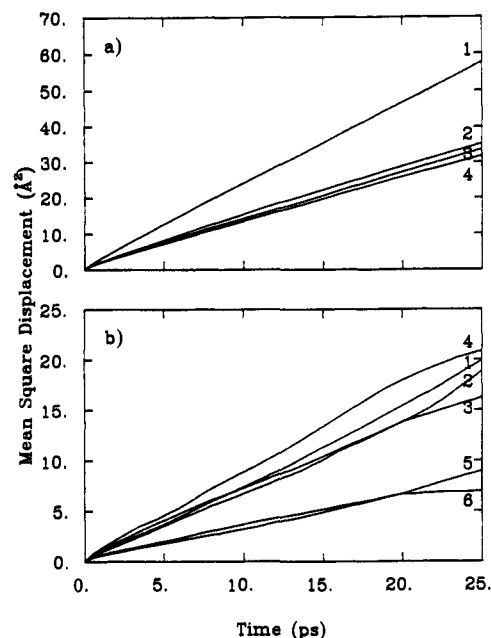


Figure 8. (a) Mean square displacements for water, 1 = aqueous DPDPE, 2 = pure salt, 3 = ions 1, and 4 = ions 2 and (b) mean square displacements for Na<sup>+</sup> ions, 1 = pure salt, 2 = ions 1, and 3 = ions 2; and Cl<sup>-</sup> ions, 4 = pure salt, 5 = ions 1, and 6 = ions 2.

The competition between the peptide and solvent for the sodium and chloride ions is dependent on the different solvation energetic properties of sodium and chloride ions. The smaller sodium ion has a high charge density and coordinates somewhat fewer overall water molecules very tightly in the first solvation shell. To interact directly with the peptide these waters of solvation would have to be disturbed. Removing one (or two) water molecule(s) is far more energetically unfavorable in the case of sodium than chloride and may explain why the sodium ions never associate strongly with the peptide. It is possible that binding of sodium ions to the carboxylate terminus is kinetically controlled involving a high barrier to activation, i.e., removal of a water molecule. After this barrier has been crossed there may be a strong interaction between sodium and carboxylate which is not observed in our simulations due to the small time period sampled.

However, in the case of the chloride ions, the first water solvation shell is larger and less tightly bound in comparison with the first solvation shell of sodium. It is easier for a water molecule to be removed from a chloride ion than from any other ion in the simulation and the lost chloride-water interaction replaced by a peptide-ion interaction. This would be especially favorable at the positively charged N terminus. The pair energy distribution for waters around chloride ions is not only lower than for sodium ions but also lower than either termini. Thus the peptide can easily displace water around chloride ions but not around sodium ions.

Similar effects have been seen before in the study of the effective adiabatic work for pairing ions of different size.<sup>29</sup> The presence of so many chloride ions in close vicinity to each other is unusual but is aided by the stabilizing effect of the peptide in conjunction with bridging water molecules.<sup>29,38</sup> This type of solvent-separated ion pair, aided by bridging water molecules, has been observed in potential of mean force calculations with various models of infinitely dilute chloride ion pairs in aqueous solution.<sup>29,38,39</sup> As alluded to earlier, this is not expected for salt water at high concentrations.

The self-diffusion constant of water was calculated for each of the four different simulations. Figure 8a shows the mean square displacement of water molecules as a function of time from which the self-diffusion constants have been extracted.<sup>50</sup> The mean square displacements were collected over 100 ps of simulation and included all water molecules. Water self-diffusion constants for

(50) Chandrasekhar, S. *Rev. Mod. Phys.* 1943, 15, 1-89.

Table II. Average Energies (rms), Temperatures, and Distances<sup>a</sup>

property	DPDPE <sup>b</sup>	ions 1	ions 2	salt
potential	-18484 (100)	-25899 (91)	-26064 (89)	-25664 (113)
kinetic	5270 (95)	4969 (90)	4907 (89)	5369 (103)
water kinetic	5065 (94)	4699 (88)	4642 (88)	5300 (103)
DPDPE kinetic	205 (24)	201 (21)	197 (21)	
ion kinetic		69 (13)	68 (13)	69 (13)
water potential	-19557 (148)	-10330 (336)	-10683 (287)	-17765 (248)
water internal	2990 (108)	2908 (103)	2901 (95)	3235 (112)
DPDPE potential	-215 (46)	-101 (33)	-118 (29)	
DPDPE-water potential	-1703 (87)	-343 (81)	-91 (70)	
DPDPE-ion potential		-3613 (100)	-3924 (84)	
ion-water potential		-19603 (537)	-19315 (431)	-10285 (303)
ion-ion potential		5184 (267)	5166 (215)	-849 (146)
water temperature	316 (6)	306 (6)	302 (6)	304 (6)
DPDPE temperature	316 (37)	310 (32)	304 (33)	
ion temperature		305 (59)	302 (58)	308 (58)
total temperature	316 (6)	306 (6)	302 (5)	304 (6)
end-to-end distance	13.13 (0.56)	10.23 (0.76)	9.69 (0.44)	

<sup>a</sup>Energies in kJ mol<sup>-1</sup>, temperatures in K, and distances in Å. <sup>b</sup>Reference 27.

the aqueous DPDPE, the pure salt, and two saline-peptide simulations were  $3.8 \pm 0.1$ ,  $2.3 \pm 0.1$ ,  $2.2 \pm 0.1$  and  $2.1 \pm 0.1 \times 10^{-9}$  m<sup>2</sup> s<sup>-1</sup>, respectively. From the above values it can be seen that the effect of ions on the self-diffusion constant of water is considerably larger than the effect of DPDPE. On exclusion of water molecules in the vicinity of DPDPE ( $\leq 6$  Å) the self-diffusion constant for the aqueous DPDPE simulation increased slightly from  $3.8$  to  $3.9 \times 10^{-9}$  m<sup>2</sup> s<sup>-1</sup>. This compares fairly well with the value of  $4.3 \times 10^{-9}$  m<sup>2</sup> s<sup>-1</sup> calculated for rigid SPC water.<sup>51</sup> Therefore, changing from a rigid SPC water model to a flexible SPC model with Ewald electrostatics does not dramatically change the resulting self-diffusion constant. This is in agreement with the result of Guardia and Padro<sup>42</sup> and Prevost et al.<sup>46</sup> but contrary to that found by Teleman et al.<sup>52</sup>

The self-diffusion constants for salt ions were calculated from Figure 8b. From the pure salt simulations we obtained values of  $1.2 \pm 0.1$  and  $1.5 \pm 0.1 \times 10^{-9}$  m<sup>2</sup> s<sup>-1</sup> for sodium and chloride ions, respectively, compared with the experimental values of  $1.3$  and  $2.0 \times 10^{-9}$  m<sup>2</sup> s<sup>-1</sup><sup>53</sup> and previous simulation results of  $0.9$ ,<sup>42</sup>  $1.5$ ,<sup>42</sup>  $1.0$ ,<sup>44</sup>  $0.7$ ,<sup>54</sup>  $1.3$ ,<sup>55</sup> and  $2.3$ ,<sup>44</sup>  $0.8$ ,<sup>54</sup>  $2.0$ ,<sup>55</sup>  $1.1$ ,<sup>56</sup>  $1.1 \times 10^{-9}$  m<sup>2</sup> s<sup>-1</sup>. From the two saline-peptide simulations we obtained values of  $1.1 \pm 0.1$  and  $1.0 \pm 0.1 \times 10^{-9}$  m<sup>2</sup> s<sup>-1</sup> for the self-diffusion constants of sodium ions and  $0.6 \pm 0.1$  and  $0.4 \pm 0.1 \times 10^{-9}$  m<sup>2</sup> s<sup>-1</sup> for chloride ions. The association between the chloride ions and DPDPE results in very low chloride ion self-diffusion constants, as also observed by Berendsen et al.,<sup>19</sup> whereas we find that the self-diffusion constant of the sodium ions remains essentially unchanged.

**(b) Conformational Properties of DPDPE in Saline Solution.** The effect of salt on various other physical properties of DPDPE was also investigated. A comparison of the energetics of the aqueous DPDPE, the two saline-peptide and the pure salt simulations is presented in Table II. The two saline-peptide simulations were remarkably similar except that in the second saline-peptide simulation there was a somewhat stronger interaction between the peptide and the ions. After equilibration (the first 100 ps), the second saline-peptide simulation gave a DPDPE structure which had three chloride ions complexed to the N terminus, whereas in the first saline-peptide simulation there were only two chloride ions complexed to the N terminus after equilibration. The third chloride ion complexed during the analysis period. Hence the second simulation had a larger average DPDPE-ion interaction and a lower average DPDPE-water in-

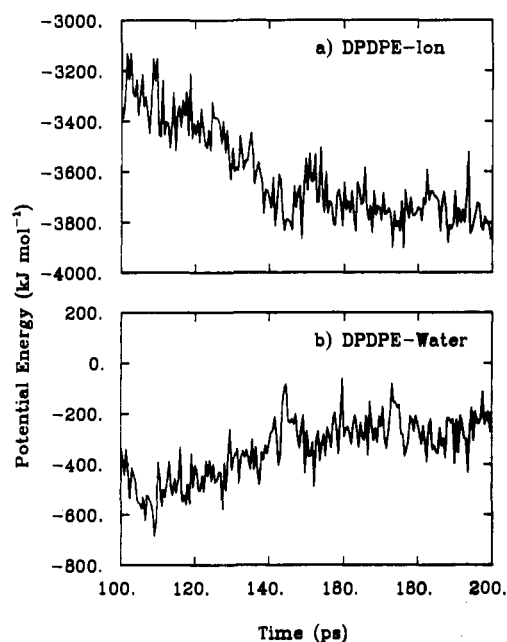


Figure 9. Potential energy time series for ions 1 showing the increasing peptide-ion interaction as the third chloride ion approaches the peptide: (a) DPDPE-ion and (b) DPDPE-water potential energies.

teraction. The approach of the third chloride ion to the peptide was evident in the DPDPE-ion and DPDPE-water potential energy time series shown in Figure 9. Here the DPDPE-ion potential energy was seen to decrease as the chloride ion approached the peptide. A corresponding, and compensating, increase in potential energy between DPDPE and the solvent was observed as the chloride ion replaced solvent molecules close to the peptide.

The large positive ion-ion potential energy in the saline-peptide simulations (Table II) was a consequence of the short chloride-chloride ion distances found in the vicinity of the N terminus. These repulsive interactions were compensated for by very favorable peptide-ion and ion-water interactions. We also noticed that the ion-water potential in the saline-peptide simulations was larger than the ion-water potential in the pure salt simulation. Correspondingly, the water-water potential was larger in the pure salt simulation compared with the two saline-peptide simulations. These differences exceed the differences expected due to the small variation in the number of water molecules in each simulation. We can explain this by considering just the chloride ions in the saline-peptide simulation. When the chloride ions are associated with the peptide, they form fewer hydrogen bonds to the solvent but are stabilized by several strongly bound bridging water molecules which are therefore relatively rigid. This means the

(51) Berendsen, H. J. C.; Grogera, J. R.; Straatsma, T. P. *J. Phys. Chem.* **1987**, *91*, 6269-6271.

(52) Teleman, O.; Jonsson, B.; Engstrom, S. *Mol. Phys.* **1987**, *60*, 193-203.

(53) Hertz, H. G. In *Water: A Comprehensive Treatise*; Franks, F., Ed.; Plenum Press: New York, 1973; Vol. 3, Chapter 7.

(54) Berkowitz, M.; Wan, W. *J. Chem. Phys.* **1987**, *86*, 376-382.

(55) Trullas, J.; Giro, A.; Padro, J. A. *J. Chem. Phys.* **1990**, *93*, 5177-5181.

(56) Reddy, M. R.; Berkowitz, M. *J. Chem. Phys.* **1988**, *88*, 7104-7110.

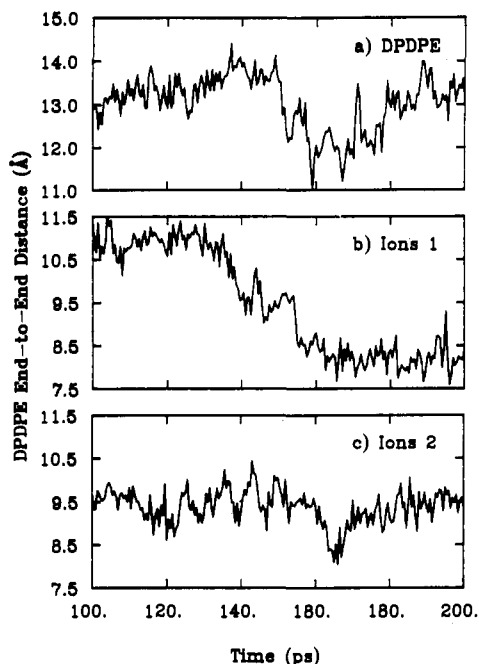


Figure 10. End-to-end distance time series for DPDPE for each of the three simulations.

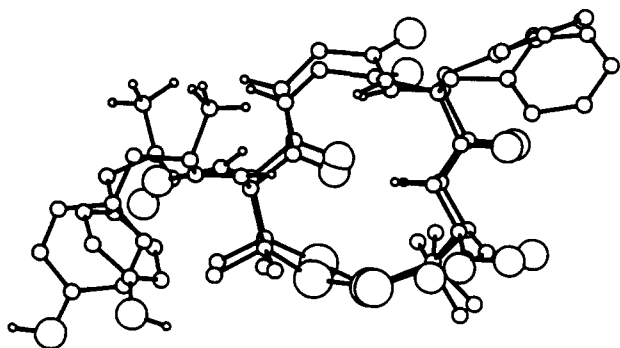


Figure 11. A comparison of the final structures of DPDPE from both saline-peptide simulations.

solvent structure surrounding the strongly bound waters is severely disrupted producing poorer water-water interactions.

The more positive DPDPE potential energies observed in the presence of ions indicated that the salt ions interacted with the peptide strongly enough to change intrapeptide interactions. Most of this strain appeared in the bond angle and electrostatic terms for DPDPE. Therefore, it appears possible for salt ions, in this case chloride ions, to distort the conformation of a peptide in solution in accord with the expectations of the Hofmeister series. In the case of DPDPE, no gross conformational changes were observed, but this is likely to be a consequence of the rather rigid (in comparison to linear peptides) cyclic nature of DPDPE. We did observe a decrease in the end-to-end distance for DPDPE in saline solution (Figure 10 and Table II). In the first saline-peptide simulation this was quite a sharp reduction near 150 ps which occurred shortly after the third chloride ion bound to the N terminus. We also observed the formation of transient  $\gamma$  and type III  $\beta$ -bends within the cyclic structure which were not observed in the aqueous simulation.<sup>27</sup> Even so, there are no sudden conformational changes, and the effects that the chloride ions had on the conformation of DPDPE were delocalized over the molecular framework. A comparison of the two conformations obtained after 200 ps of simulation in saline solution is shown in Figure 11. This figure illustrates the remarkable similarity of the two 200-ps simulations which started from different initial configurations.

An interesting feature of the simulations was the presence of a long time oscillation in the end-to-end distance time series which

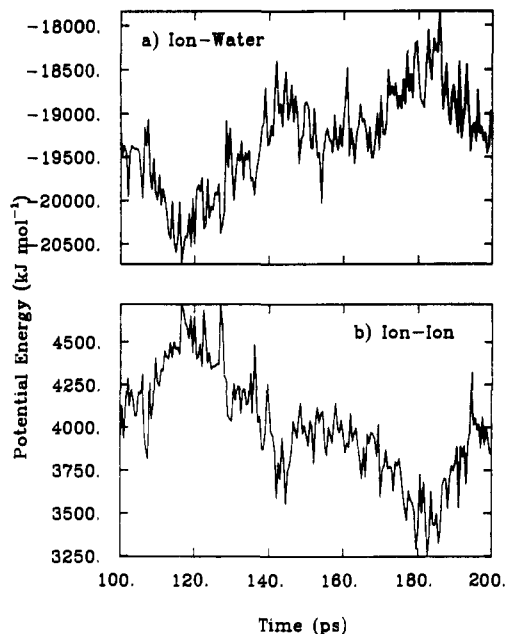


Figure 12. Potential energy time series for (a) ion-water and (b) ion-ion interactions. Note the low-frequency oscillation with a period of almost exactly 100 ps.

Table III. Initial and Final Dihedrals

dihedral	initial <sup>a</sup> (0 ps)	DPDPE <sup>b</sup> (250 ps)	ions 1 (200 ps)	ions 2 (200 ps)
$\psi_1$	163	168	66	81
$\chi_1^1$	-163	-72	-162	-143
$\chi_1^2$	51	-107	-161	-43
$\chi_1^3$	-179	12	175	-150
$\phi_2$	111	85	138	155
$\psi_2$	13	-147	-62	-59
$\chi_2^1$	180	-177	-141	-152
$\chi_2^2$	143	122	97	105
$\chi_2^3$	-110	-162	-132	-129
$\phi_3$	-98	91	-52	-35
$\psi_3$	-18	-62	-35	-29
$\phi_4$	-72	-90	-88	-98
$\psi_4$	-46	-28	-26	-31
$\chi_4^1$	179	-80	-159	-168
$\chi_4^2$	68	-89	-167	70
$\phi_5$	83	90	89	106
$\psi_5$	56	54	65	72
$\chi_5^1$	-70	-47	-66	-69
$\chi_5^2$	119	123	133	125

<sup>a</sup> Reference 24. <sup>b</sup> Reference 27.

also appeared in the ion-water and ion-ion potential energy time series (Figure 12). An oscillation of almost exactly 100 ps was clearly evident in all these properties. As mentioned previously,<sup>27</sup> this type of long time oscillation has also been observed for myoglobin in water.<sup>57</sup> It appears that this feature is independent of the box size and the peptide size and is observed in several different systems. The origin of this oscillation is probably a long time collective motion of water although the exact nature of this motion remains somewhat unclear at present.

Table III contains the final dihedral angles of DPDPE from each of the simulations. Except for  $\psi_1$  the two saline-peptide simulations produced structures which had essentially identical main chain dihedral angles. In the case of  $\psi_1$  the binding of the chloride ions to the peptide distorted this dihedral producing a structure where chloride ions were bound to an N terminal hydrogen and an amide hydrogen simultaneously. This elastic distortion occurred during the equilibration period and was stable throughout the rest of the simulation. We did not observe any transitions around the tyrosine  $\chi^1$  during the saline-peptide simulations unlike the aqueous simulation where the tyrosine side chain flipped from a t to a g<sup>-</sup> conformation.<sup>27</sup> The presence of the salt ions in the vicinity of the N terminus could have quite

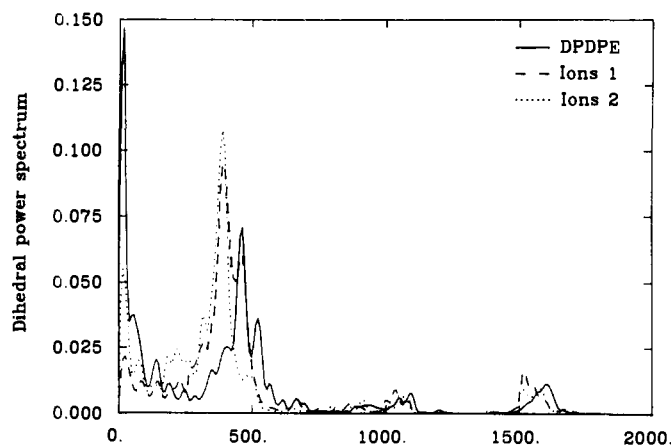


Figure 13. The dihedral power spectra for dihedrals which contain the N terminal hydrogens. The spectra have been normalized so as the total area under each spectrum is unity.

a pronounced effect on this type of transition although the total time of the simulations is insufficient to sample all the possible rotamers with the equilibrium populations.

The second saline-peptide simulation, in which three chlorides were associated with the N terminus, displayed no dihedral transitions during the 100 ps of analysis. In the first simulation we observed some ring rotation in the tyrosine residue as was also observed in the pure water simulation. An amide flip, involving correlated rotation about  $\psi_3$  and  $\phi_4$ , was also observed before the third chloride ion complexed to the peptide. After the third chloride ion bound to the peptide, no further transitions were observed. Although very few main chain dihedral transitions were observed, there was a gradual change in several dihedrals of approximately 20–30 deg. This elastic deformation could explain the decrease in the end-to-end distance even though no large conformational transitions were found.

We compared the velocity autocorrelation functions and their corresponding power spectra for the solvent and the peptide obtained from the last 10 ps of each of the simulations. The water spectra displayed no significant differences between simulations, but this is probably due to the fact that the small experimental shifts observed ( $\approx 20 \text{ cm}^{-1}$ )<sup>58</sup> in salt solutions are of the same order of magnitude as our spectral resolution. However, the dihedral autocorrelation function power spectra did show some interesting differences. The power spectra of the dihedral autocorrelation function for dihedrals which include the N terminal hydrogens are shown in Figure 13. We observed a shift to lower frequencies for several peaks in both saline-peptide simulations. The peak at  $467 \text{ cm}^{-1}$  in the aqueous simulation was red-shifted to  $383 \text{ cm}^{-1}$  with a corresponding increase in intensity. This effect was also seen for the peak at  $1600 \text{ cm}^{-1}$  which was shifted to  $1517 \text{ cm}^{-1}$ . Both of these shifts were significantly larger than our spectral resolution of  $17 \text{ cm}^{-1}$ . The observed shifts to lower frequencies are consistent with an increase in effective mass of the N terminal hydrogens on association of the chloride ions.

Another feature of the saline-peptide simulations was the appearance of a peak at  $300 \text{ cm}^{-1}$  in the power spectrum of the  $\phi_3$  dihedral (Figure 14). A peak at  $300 \text{ cm}^{-1}$  was also observed in the sodium ion power spectrum (Figure 15). It is unclear if there was any energy exchange between the sodium ions and the atoms of the  $\phi_3$  dihedral although this seems unlikely due to the lack of any close contacts between the peptide and any sodium ions. A more satisfactory explanation of the new frequency was the presence of a transient type III  $\beta$ -bend between the carbonyl group of D-Pen-2 and the amide hydrogen of D-Pen-5 (shown in Figure 11). This transient hydrogen bond could have given rise to the new low-frequency motion as no intrapeptide hydrogen bonds, permanent or transient, were seen in the aqueous simulation.<sup>27</sup>

#### IV. Conclusions

The simulations presented above suggest that there is the possibility of a degree of anion association with DPDPE in saline

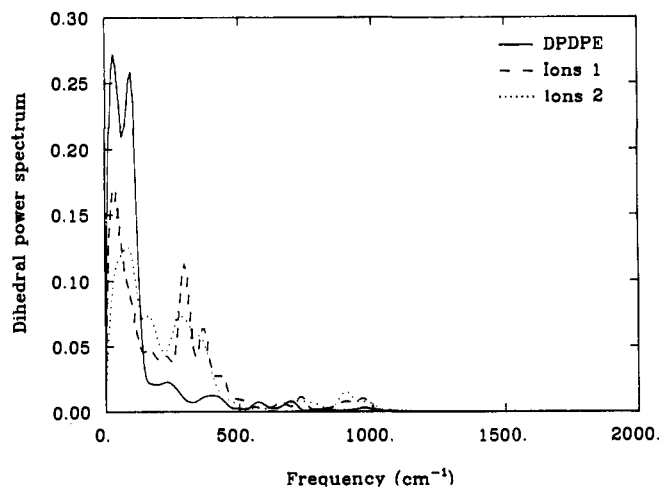


Figure 14. The  $\phi_3$  dihedral power spectra. The spectra have been normalized so as the total area under each spectrum is unity.

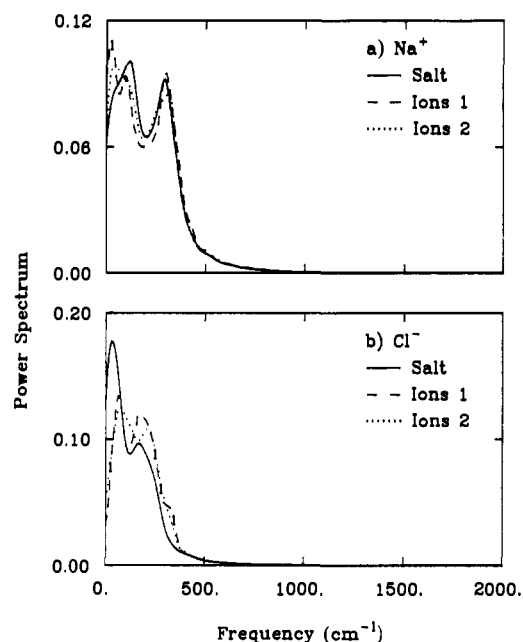


Figure 15. Power spectra of the velocity autocorrelation functions for (a)  $\text{Na}^+$  and (b)  $\text{Cl}^-$  ions. The spectra have been normalized so as the total area under each spectrum is unity.

solution. In comparison, there appears to be no association between the cations and the peptide. The preferential association of chloride ions has been rationalized by reference to the electrostatic potential energy of DPDPE and the relative strength of binding of water to the salt ions versus the ionic centers of the peptide. Chloride ions associate with the positive N terminus with additional interactions to nearby amide hydrogens. There are as many as three chloride ions associated with the ammonium group, one hydrogen bonded to each of the hydrogen atoms mutually bridged by water molecules. This binding is stable over the duration of both simulations. The similar results obtained from the two different simulations suggest the observations are robust and independent of the initial positioning of the sodium and chloride ions.

One of the results of ion association is to modify the relative positions of the N terminus and its neighboring amide hydrogens in order to facilitate multiple hydrogen bonding to the chloride ions. The major conformational changes are the decrease in the  $\psi_1$  dihedral and a decrease in end-to-end distance which is accompanied by the formation of a transient, hydrogen-bonded, type III  $\beta$ -bend within the cyclized DPDPE structure. In comparison, no type III  $\beta$ -bends were observed for DPDPE in aqueous solution.<sup>24,27</sup> If the results from this simulation of a molecular model



are qualitatively correct, the strong association between chloride anions and a peptide would be expected for other zwitterions, or residues with positively charged side chains, and maybe even neutral peptide groups. If this is so, the possible effects of the specific association of ions on peptide conformation will considerably complicate a number of present computationally convenient modeling techniques.

Timasheff and Arakawa have found that the salting-out of proteins can be decomposed into two contributions.<sup>59</sup> One from nonspecific preferential exclusion of the cosolvent from the protein surface and one from the specific binding of the ligand to the protein. The balance between these two effects leads to either solubilization or precipitation. Within the cations Na<sup>+</sup>, Mg<sup>2+</sup>, Ca<sup>2+</sup>, Ba<sup>2+</sup> and guanidinium, sodium had the highest preferential exclusion while for the anions Cl<sup>-</sup>, AcO<sup>-</sup>, and SO<sub>4</sub><sup>2-</sup>, chloride ion was the least preferentially excluded.<sup>59</sup> This is certainly in agreement with the simulations described here. In addition, Arakawa and Timasheff also observed the binding of NaCl to  $\beta$ -lactoglobulin and attributed this binding to the large dipole moment of the protein.<sup>60</sup> As chloride ions are the least preferentially excluded and sodium ions the most preferentially excluded from the protein surface,<sup>59</sup> this suggests binding of the chloride ions to  $\beta$ -lactoglobulin. These observations are again in agreement with the above simulations.

From these simulations it is not possible to gain any real insight into the relative binding of other ions. This will only be possible by further simulations with different salts. However, in the case studied here the effects are dominated by anions with the cations acting as spectator ions.

**Acknowledgment.** We thank Prof. Victor J. Hruby, Dr. Fahad Al-Obeidi, and Dr. James M. Briggs for numerous interesting discussions and the Robert A. Welch Foundation and the National Institutes of Health for partial support. Finally we thank the San Diego Supercomputer Center for generous use of their Cray X-MP and Y-MP machines.

## Appendix

The Ewald potential<sup>31</sup> for a system of  $N$  atoms each carrying a charge,  $q$ , in a box of length,  $L$ , surrounded by a medium of

(57) Finsen, L. A.; Subramanian, S.; Pettitt, B. M. *Biophys. J.* Submitted for publication.

(58) Verrall, R. E. In *Water: A Comprehensive Treatise*; Franks, F., Ed.; Plenum Press: New York, 1973; Vol. 3, Chapter 5.

(59) Timasheff, S. N.; Arakawa, T. *J. Cryst. Growth* 1988, 90, 39-46.

(60) Arakawa, T.; Timasheff, S. N. *Biochemistry* 1987, 26, 5147-5153.

dielectric,  $\epsilon'$ , is given by<sup>32</sup>

$$V(r, \epsilon') = \sum_{1 < i < j \leq N} q_i q_j \psi(r_{ij}) + \frac{\xi}{2} \sum_{i=1}^N q_i^2 + \frac{2\pi}{(2\epsilon' + 1)L^3} \left| \sum_{i=1}^N q_i r_i \right|^2 \quad (1)$$

where

$$\psi(r) = \sum_{|n|=0}^{\infty} \frac{\operatorname{erfc}(\kappa|r + nL|)}{|r + nL|} + \frac{1}{\pi L} \sum_{|n| \neq 0} \frac{1}{|n|^2} \exp\left(\frac{2\pi i}{L} \mathbf{n} \cdot \mathbf{r} - \frac{\pi^2 |n|^2}{\kappa^2 L^2}\right) \quad (2)$$

with

$$\xi = \sum_{|n| \neq 0} \left[ \frac{\operatorname{erfc}(\kappa|nL|)}{|nL|} + \frac{1}{\pi L |n|^2} \exp\left(-\frac{\pi^2 |n|^2}{\kappa^2 L^2}\right) \right] - \frac{2\kappa}{\sqrt{\pi}} \quad (3)$$

and

$$\operatorname{erfc}(x) = 1 - \frac{2}{\sqrt{\pi}} \int_0^x \exp(-t^2) dt \quad (4)$$

The sum over the lattice vectors,  $n_x$ ,  $n_y$  and  $n_z$  is performed for all  $|n| \leq 4$  which produces a spherical arrangement of 256 images around the central box. We used a value of  $\kappa = 2.25/L$  with the so-called conducting, or "tin foil", boundary conditions ( $\epsilon' = \infty$ ). Due to the computationally intensive nature of the Ewald sum a table lookup procedure was employed in our simulations. The Ewald potential, and its analytic first and second derivatives, were stored on a  $50 \times 50 \times 50$  grid placed on the central box, and a cubic interpolation of the potential and a quartic interpolation of the force were then implemented to obtain the potential and force for a given interatomic separation.

Our simulations called for an infinitely dilute solution of DPDPE. This was achieved by skipping the interaction of DPDPE with its images in the surrounding periodic boxes. This results in the presence of a cavity in the periodic images. However, this did not seem to have any inadvertent effects on the dynamics of the system. As a check we performed a short finite concentration simulation of DPDPE by including the Ewald terms for all peptide-peptide image electrostatic interactions. There was no significant deviation in the structure or dynamics of the peptide or solvent from that obtained at infinite dilution.

Registry No. DPDPE, 88373-73-3; NaCl, 7647-14-5.

## QCFF/PI Vibrational Frequencies of Some Spherical Carbon Clusters

Fabrizia Negri, Giorgio Orlandi, and Francesco Zerbetto\*

Contribution from the Dipartimento di Chimica "G. Ciamician", Universita' di Bologna, Via F. Selmi 2, 40126 Bologna, Italy. Received January 4, 1991

**Abstract:** QCFF/PI calculations of the vibrational frequencies of C<sub>60</sub>, C<sub>70</sub>, and the two highest symmetry C<sub>84</sub> carbon clusters are presented. The results should be of help in the assignment of the vibrational spectra of the newly isolated carbon clusters and possibly in determining the structure of C<sub>84</sub>. The agreement between the calculated and the experimentally available frequencies is remarkable with the largest discrepancies of 30 cm<sup>-1</sup> for C<sub>60</sub> and 65 cm<sup>-1</sup> for C<sub>70</sub>. It is proposed that the QCFF/PI method be the method of choice to obtain the vibrational frequencies of fullerene molecules.

## Introduction

Very recently the long quest for the C<sub>60</sub> and C<sub>70</sub> carbon clusters was met with success.<sup>1</sup> The two molecules were isolated and shown to have fullerene structure through the analysis of their

NMR spectra.<sup>2</sup> Their full infrared, Raman, and UV characterization is now in progress.<sup>3</sup> It can be hoped that very soon

(2) Taylor, R.; Hare, J. P.; Abdul-Sada, A. K.; Kroto, H. W. *J. Chem. Soc., Chem. Commun.* 1990, 1423-1425.

(3) Bethune, D. S.; Meijer, G.; Tang, W. C.; Rosen, H. J. *Chem. Phys. Lett.* 1990, 174, 219-222.

(1) Kratschmer, W.; Lamb, L. D.; Fostiropoulos, K.; Huffman, D. R. *Nature* 1990, 347, 354-358.